Ultrafast Magnetization Reversal Dynamics Investigated by Time Domain Imaging

B. C. Choi, M. Belov, W. K. Hiebert, G. E. Ballentine, and M. R. Freeman
Department of Physics, University of Alberta, Edmonton, Alberta, Canada T6G 2J1
(Received 11 July 2000)

Spatiotemporal magnetization reversal dynamics in a $Ni_{80}Fe_{20}$ microstructure is studied using ps time scale scanning Kerr microscopy. Time domain images reveal a striking change in the reversal associated with the reduction in switching time when a transverse bias field is applied. Magnetization oscillations subsequent to reversal are observed at two resonance frequencies, which sensitively depend on the bias field strength. The oscillation at $f = 2$ GHz is caused by the damped precession of **M**, while the lower frequency ~0.8 GHz mode is interpreted in terms of domain wall oscillation.

DOI: 10.1103/PhysRevLett.86.728 PACS numbers: 75.60.Ch, 75.70.Ak, 75.70.Kw, 78.20.Ls

From both fundamental and application points of view, the switching time required for the magnetization reversal is of utmost significance. While magnetization reversal in micro- and nanosized magnets has been actively studied recently [1–5], a clear view of the reversal dynamics has not been achieved experimentally. In the case of quasistatic magnetic configurations, magnetic force, Bitter pattern, and other microscopies provide highly detailed results [6,7]. These techniques, however, do not offer enough temporal resolution to observe a real time switching process. For the investigation of reversal dynamics it has been demonstrated that time-resolved scanning Kerr microscopy is a powerful tool [8–12], allowing direct insight into the spatiotemporal evolution of the switching process.

In this Letter, we present the ps time scale stroboscopic [13] scanning Kerr microscopy experiments on a 15 nm thick polycrystalline $Ni_{80}Fe_{20}$ structure (10 μm × 2 μm), patterned by electron beam lithography. During the film growth, an in-plane magnetic field was applied to induce a uniaxial anisotropy. The measured coercivity H_c along the easy axis of the patterned structure is 1.3 kA/m, and the hard-axis saturation field of 3.8 kA/m corresponds to the anisotropy field. The $Ni_{80}Fe_{20}$ structures are made on a 20 μm wide and 300 nm thick gold transmission line that carries a fast current pulse. The current creates an in-plane switching field (H_s) of 24 kA/m along the long axis of the sample with 0.5 ns rise time, 1.5 ns fall time, and 10 ns duration [14]. The current pulses are synchronously triggered by a mode-locked Ti-sapphire fs laser ($\lambda = 800$ nm, 0.8 MHz repetition rate). Magnetization measurements are accomplished through polarization analysis of the reflected light in an optical bridge with quadrant detectors [14]. In the present experiment a 180° reversal configuration was used [Fig. 1(a)]. The sample is first saturated in the x direction by an in-plane bias field H_l, and then a switching pulse H_s is applied antiparallel to H_l in order to flip the magnetization. Additionally, an in-plane transverse bias field H_t is applied along the hard axis of the sample to manipulate the switching time and magnetization reversal processes.

Figure 1(b) represents the time dependence of the magnetization component M_x along the easy axis, measured in the center of the structure for different H_t, while H_l is kept at 4.8 kA/m. For $H_t = 0$ kA/m, a definite delay in the magnetic response after the beginning of the pulse is observed. The subsequent dynamics are relatively slow with the magnetization fully reversed after ~3.5 ns. Furthermore, the asymmetry between front and back reversal

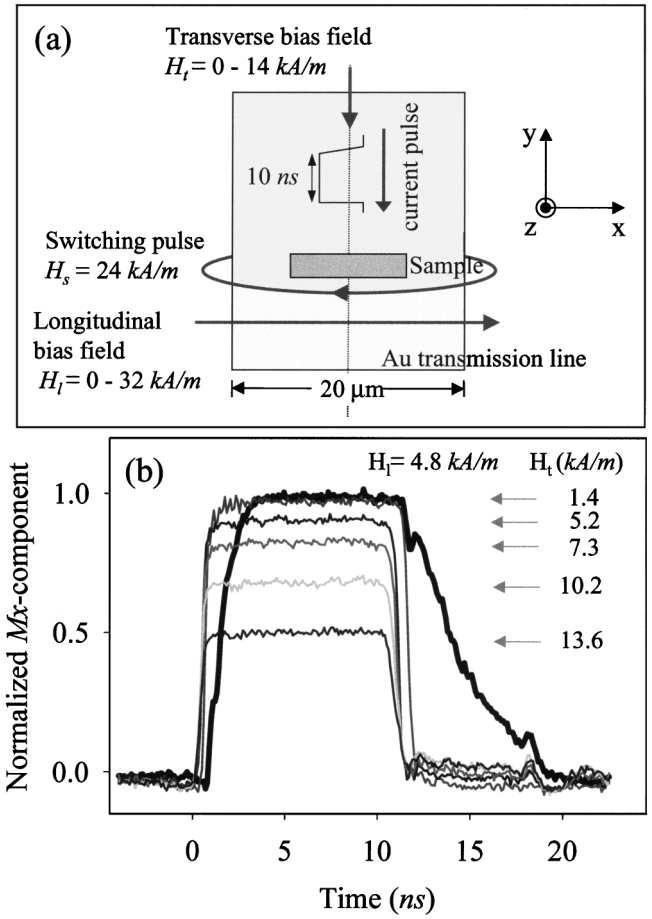

FIG. 1. (a) Schematic configuration for 180° dynamic reversal experiments. H_s, H_l, and H_t indicate the switching, easy-axis bias, and hard-axis bias fields. (b) Time-resolved M_x component measured at the center of the element for different H_t, at H_l = 4.8 kA/m. The switching pulse begins at 0 ns. The thick line indicates the M_x component measured at $H_t = 0$ kA/m.

 0031-9007/01/86(4)/728(4)$15.00

is pronounced, owing to different net switching fields H_s^{net} driving the switching in the two cases (19.2 kA/m for the forward and 4.8 kA/m for the back reversal). Under these field conditions we find $\tau_s = 1.6$ and 7.3 ns for forward and back switching, respectively, defining switching time τ_s as the interval for 10% to 90% of the total M_x change. We note that these times are roughly consistent with the prediction of a rotational model [15,16] in which τ_s is related to H_s^{net} by the equation $\tau_s = S_w/H_s^{\text{net}}$, where S_w is the switching coefficient. From the data in Fig. 1(b) S_w is found to be ~ 30 A $\cdot$ μs/m (somewhat larger than 16 A $\cdot$ μs/m reported in Ref. [16]), but in addition we find that the inverse relation is not strictly obeyed over a broader field range [17]. These differences are attributable to measuring a "local" τ_s at the sample center instead of an average over the whole sample.

A remarkable difference in the reversal is found by applying a transverse bias field H_t. When H_t is applied, the sample responds earlier to the switching pulse. Correspondingly, the rise time rapidly decreases and the magnetization reverses within 1 ns after the beginning of the pulse. A field strength as low as $H_t = 1.4$ kA/m was found to be sufficient to cause such an abrupt switching. The fast switching can be understood as follows: If H_t is applied, the effective H_c is lower than the case where $H_t = 0$ kA/m. This situation arises because for a finite H_t the equilibrium position of **M** is away from the easy axis, the position of minimum anisotropy energy. Thus, lower longitudinal Zeeman energy or smaller H_s is required to overcome the energy barrier. We note that this drastic change in switching behavior is also reflected in hysteresis loops (not shown), which manifest a decrease in H_c from 1.3 to 1.0 kA/m and increase in squareness in the presence of H_t [17].

The effect of applying H_t is directly examined through time domain images taken during the reversal. Figure 2 shows a sequence of frames showing the change of M_x. For $H_t = 0$ kA/m, the reversal is mainly governed by a domain nucleation process. In the very beginning ($t = 0.5$ ns) a stripelike instability is observed inside the sample, from nucleation occurring in the same regions. The main dynamical reversal, however, is first initiated from the demagnetized edges (0.9 ns), is followed by expansion of the nucleated domains (1.3 and 2.1 ns), and finally leads to a uniform distribution of fully reversed magnetization, excluding the left and right edge regions (5 ns). These edge regions correspond to free magnetic poles related to the demagnetized areas in a ferromagnet of finite size. On the back reversal, the stripe instability is also pronounced (12.2 ns). From this result, it becomes clear how the switching [Fig. 1(b)] evolves spatiotemporally: The finite domain nucleation limits switching time to ~ 3.5 ns.

It is this nucleation-dominant reversal process which is manipulated through application of H_t. Applying $H_t = 5.2$ kA/m, the 180° domains at the short edges are formed

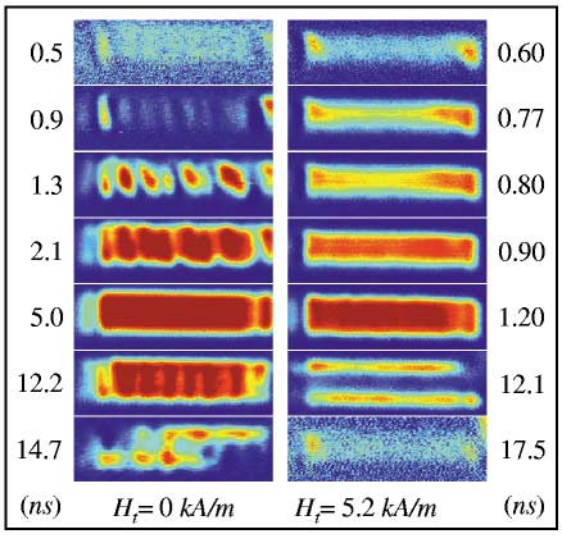

FIG. 2 (color). Spatial profile of the M_x component as a function of time (ns) after the magnetic pulse was applied. $H_l = 4.8$ kA/m, while the transverse field are varied $H_t = 0$ and 5.2 kA/m. The field of view of each frame is 12×4 μm and contains the entire 10×2 μm sample.

(0.6 ns), but there appears no stripelike distribution inside. The edge domains expand quickly in the easy axis direction to form a long, narrow domain parallel to the easy axis (0.77 ns). In the next stage, this elongated domain expands by parallel shifts in the hard direction towards the long edge (0.8 and 0.9 ns) until saturation is reached (1.20 ns). This type of reversal, which is characteristic of domain wall motion, is considerably faster as revealed in the time dependence of magnetization in Fig. 1(b). The differences in the time domain sequences shown in Fig. 2 demonstrate that the formation of nuclei inside the sample is avoided in the presence of H_t and that the nucleation process is replaced by domain wall motion. Switching occurs over longer times when the stripe domains are involved in the reversal process than if pure domain wall motion occurs.

Another aspect of reversal concerns the time scale and mechanism for removal of the initial excess Zeeman energy from the system. Coherent oscillations of the magnetization **M** may be observable after the direction has reversed, in cases where the damping is not too strong and where the energy has not propagated into a spin wave manifold which averages incoherently over the spatial resolution of the measurement (so-called "indirect damping" [18]). In these experiments, this regime is encountered when **M** is pulsed by H_s in the presence of a high H_l and moderate strength H_t. Figure 3 shows the time-resolved M_x for different H_l with $H_t = 5.2$ kA/m. Two distinct resonance frequencies are found depending on H_l. First, small oscillations at $f \sim 2$ GHz are found for $H_l = 8.8$–10.4 kA/m. It is also visible that the amplitudes at $H_l = 8.8$ and 9.6 kA/m rapidly decrease with increasing time. We treat this oscillation as damped ferromagnetic resonance about the

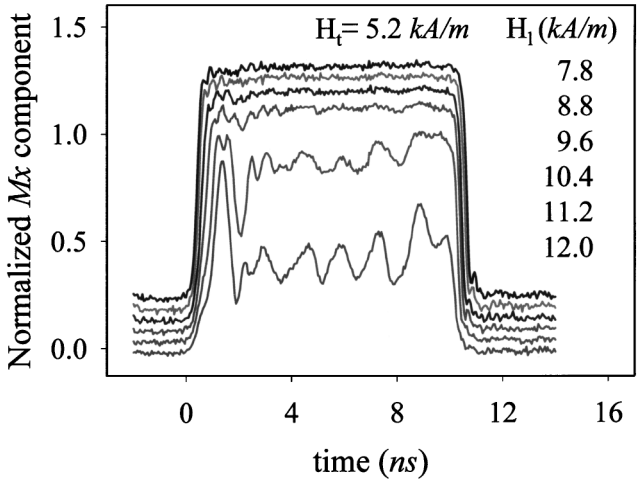

FIG. 3. Time-resolved M_x component at the center of the element for different H_l with $H_t = 5.2$ kA/m. The vertical scale is normalized by M_s measured at $H_l = 7.8$ kA/m, and the data are offset vertically in order to compare the oscillation behavior directly.

new equilibrium direction to infer the saturation magnetization M_s through $f = \gamma\mu_0(H_t M_s)^{1/2}/2\pi$ (derived from the Landau-Lifshitz equation [5]). Using the previously determined value [9] $\gamma = 1.41 \times 10^5$ m/s · A yields $\mu_0 M_s = 820$ kA/m, close to the bulk value 864 kA/m for $Ni_{80}Fe_{20}$.

When H_l increases beyond 10.4 kA/m, an oscillation with another frequency occurs, and well-developed oscillations are found at $H_l = 11.2$ and 12 kA/m. This type of oscillation is characteristically a first "spike" followed by a series of smaller oscillations. The spike is an overshoot associated with the application of H_s, with over-rotation past what will become the new equilibrium magnetization direction also apparent in the M_y component (not shown) [17]. Some of the excess energy associated with this overshoot subsequently devolves to the new oscillation mode, with a typical frequency of ~0.8 GHz, much lower than that of the previous oscillation.

An in-depth understanding of this low-frequency resonance is obtained from the spatiotemporal magnetization profiles. The lower part of Fig. 4 shows frames from an imaging sequence through one cycle of oscillation taken with bias fields, $H_l = 11.2$ kA/m and $H_t = 5.2$ kA/m. An expanded view of the oscillation measured along the easy axis is shown in the upper part of Fig. 4. The first interesting point found in the spatial profiles is the pronounced asymmetrical shift of the demagnetizing regions in the hard direction. This asymmetry is attributed to the transversal shift of the free magnetic poles at the short edges, which is caused by the additional demagnetizing field in the transverse direction. The frame at 4.55 ns corresponds to the magnetic configuration for the peak, indicated by the arrow [1]. In accordance with the magnetization curve at $H_l = 11.2$ kA/m in Fig. 3, no complete

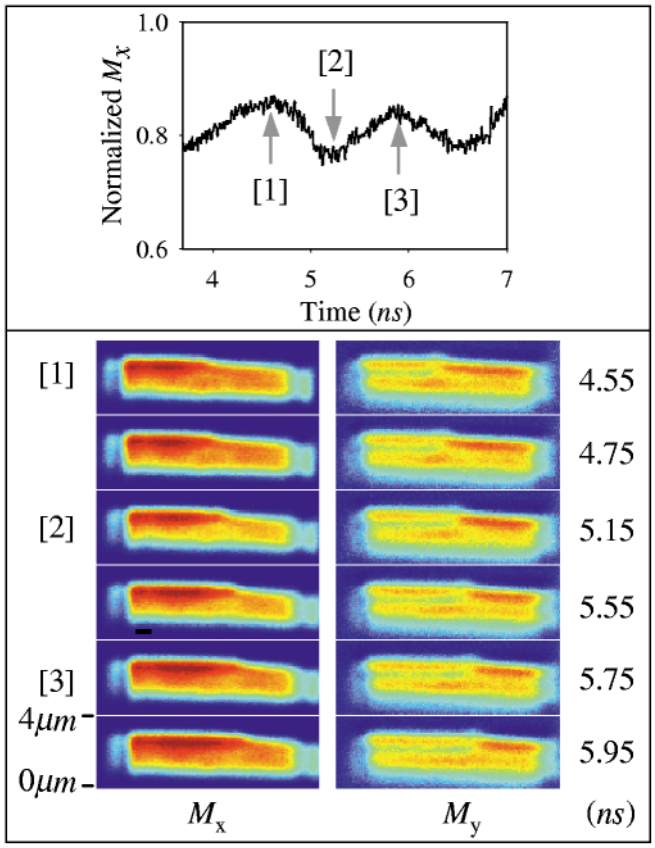

FIG. 4 (color). Time-resolved M_x component and spatial profile of M_x and M_y components as a function of time with $H_l = 11.2$ kA/m and $H_t = 5.2$ kA/m. The spatial profile frames span one oscillation period, as shown with marks on the time trace indicating the positions for the time domain images.

reversal occurs since the sample could not be fully saturated. As a result, a single-domain state cannot be persistent at this bias field, and the usual precession condition in the saturated sample, like the oscillation at $f = 2$ GHz, will not hold. This situation is found in the frames from $t = 4.55$ to 5.75 ns, spanning one oscillation period. A striking observation is the directional movement of the elongated domain in the hard-axis direction, which is different from the more symmetrical shift of the elongated domain seen from $t = 0.77$ to 0.90 ns in the right column of Fig. 2. According to the domain images over a cycle, the domain evolution in Fig. 4 is characterized as a repetitive expansion and withdrawal of elongated domains in the short axis directions, accompanied by a gradual propagation of the domain along the long axis. The continuous domain propagation is responsible for the continuous increase of the M_x intensity as observed for $H_l = 11.2$ and 12 kA/m in Fig. 3, whereas the periodic movement of domain wall in the hard-axis direction results in the low frequency ($f \approx 0.8$ GHz) oscillation. Supporting this view, M_y exhibits little change during the oscillation (right side panel in Fig. 4), except that the M_y intensity in the upper-right side of the profile gradually decreases due to the propagation of the M_x domain toward the right.

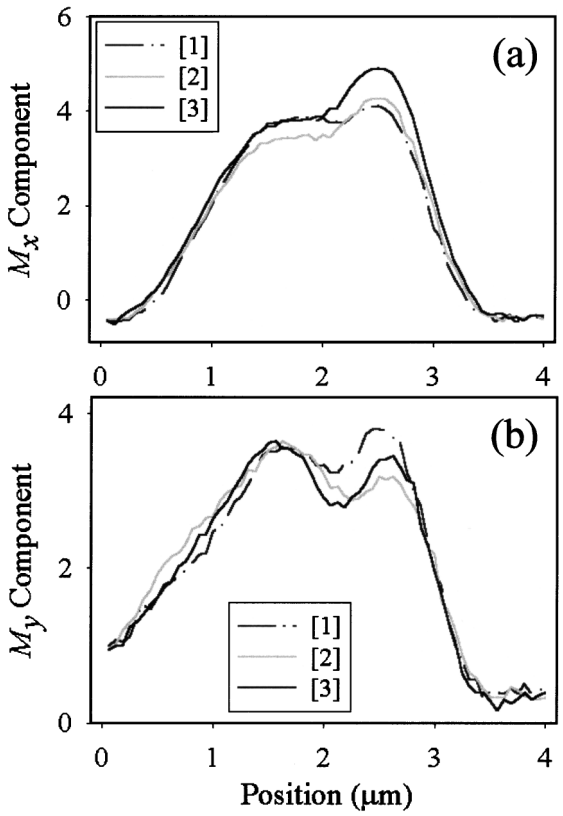

FIG. 5. Cross sections of M_x (a) and M_y (b) components measured at the middle line of the spatial profiles in Fig. 4 for $t = 4.55$, 5.15, and 5.75 ns. The x scale corresponds to the position as indicated at the lower-left frame in Fig. 4.

These sensitive changes are better visualized with the cross sections of the spatial profiles. Figure 5 clearly demonstrates that M_x oscillates at the domain wall region (around 1.5 μm on the abscissa), while M_y remains constant. This indicates that the observed oscillation in Fig. 4 originates from domain movement and not from the precession of **M**. The oscillation amplitude is small relative to our spatial resolution; hence it is manifested in the signal primarily as an amplitude change rather than a spatial displacement. From the focus spot size of 0.8 μm in diameter, a domain wall velocity of 0.12 km/s is estimated from the change of the M_x intensity. This value is much lower than the predicted Walker velocity [19,20] of $\sim$3 km/s, above which an oscillating regime is added to a constant domain wall velocity.

In summary, a complete picture of the dynamic magnetization reversal in a $Ni_{80}Fe_{20}$ microstructure has been obtained experimentally through time-resolved Kerr microscopy. The application of a transverse bias field H_t leads to an abrupt drop in the switching time and completely changes the magnetization reversal mode. Furthermore, two distinct oscillation behaviors, a precessional magnetization motion and a domain wall oscillation, are found after the magnetization is reversed by the switching field.

We acknowledge support from the Natural Sciences and Engineering Research Council of Canada, the Canadian Institute for Advanced Research, and the National Storage Industry Consortium. The samples were produced at the University of Alberta MicroFab, and the measurements were performed on equipment donated by Quantum Corp.

[1] C. H. Back, D. Weller, J. Heidmann, D. Mauri, D. Guarisco, E. L. Garwin, and H. C. Siegmann, Phys. Rev. Lett. **81**, 3251 (1998).
[2] C. Stamm, F. Marty, A. Vaterlaus, V. Weich, S. Egger, U. Maier, U. Ramsperger, H. Fuhrmann, and D. Pescia, Science **282**, 449 (1998).
[3] M. Hehn, K. Ounadjela, J.-P. Bucher, F. Rousseaux, D. Decanini, B. Bartenlian, and C. Chappert, Science **272**, 1782 (1996).
[4] R. P. Cowburn, D. K. Koltsov, A. O. Adeyeye, M. E. Welland, and D. M. Tricker, Phys. Rev. Lett. **83**, 1042 (1999).
[5] R. H. Koch, J. G. Deak, D. W. Abraham, P. L. Trouilloud, R. A. Altman, Yu Lu, W. J. Gallagher, R. E. Scheuerlein, K. P. Poche, and S. S. P. Parkin, Phys. Rev. Lett. **81**, 4512 (1998).
[6] H. Koo, T. V. Luu, R. D. Gomez, and V. V. Metlushko, Appl. Phys. Lett. **87**, 5114 (2000).
[7] J. Shi, S. Tehrani, T. Zhu, Y. F. Zheng, and J.-G. Zhu, Appl. Phys. Lett. **74**, 2525 (1999).
[8] A. Y. Elezzabi, M. R. Freeman, and M. Johnson, Phys. Rev. Lett. **77**, 3220 (1996).
[9] W. K. Hiebert, A. Stankiewicz, and M. R. Freeman, Phys. Rev. Lett. **79**, 1134 (1997).
[10] T. M. Crawford, T. J. Silva, C. W. Teplin, and C. T. Rogers, Appl. Phys. Lett. **74**, 3386 (1999).
[11] G. Yu, A. V. Nurmikko, R. F. C. Farrow, R. F. Marks, M. J. Carey, and B. A. Gurney, Phys. Rev. Lett. **82**, 3705 (1999).
[12] G. E. Ballentine, W. K. Hiebert, A. Stankiewicz, and M. R. Freeman, J. Appl. Phys. **87**, 6830 (2000).
[13] Although the stroboscopic measurements yield mainly the repetitive aspects of the dynamics, evidence of additional random behavior has not been seen in the present work [see M. R. Freeman, R. A. Hunt, and G. M. Steeves, Appl. Phys. Lett. **77**, 717 (2000)].
[14] M. R. Freeman and W. K. Hiebert, in "Spin Dynamics in Confined Magnetic Structures," edited by B. Hillebrands and K. Ounadjela (Springer-Verlag, Berlin, Heidelberg, to be published).
[15] E. M. Gyorgy, J. Appl. Phys. **29**, 283 (1958).
[16] F. B. Humphrey, J. Appl. Phys. **29**, 284 (1958).
[17] B. C. Choi, G. E. Ballentine, M. Belov, W. K. Hiebert, and M. R. Freeman (to be published).
[18] M. Ramesh, E. Jedryka, P. E. Wigen, and M. Shone, J. Appl. Phys. **57**, 3701 (1985).
[19] J. H. Spreen and B. E. Argyle, J. Appl. Phys. **53**, 4315 (1982); B. E. Argyle, W. Jantz, and J. C. Slonczewski, J. Appl. Phys. **54**, 3370 (1983).
[20] M. Cyrot, *Magnetism of Metals and Alloys* (North-Holland Publishing Company, Amsterdam, 1982), 1st ed.